Hindawi
Journal of Electrical and Computer Engineering
Volume 2023, Article ID 9898371, 1 page
https://doi.org/10.1155/2023/9898371

Retraction

Retracted: Design and Research of Building Indoor Environment Monitoring System Relying on 3D Modeling and Image Processing

Journal of Electrical and Computer Engineering

Received 19 December 2023; Accepted 19 December 2023; Published 20 December 2023

This article has been retracted by Hindawi following an investigation undertaken by the publisher [1]. This investigation has uncovered evidence of one or more of the following indicators of systematic manipulation of the publication process:

(1) Discrepancies in scope
(2) Discrepancies in the description of the research reported
(3) Discrepancies between the availability of data and the research described
(4) Inappropriate citations
(5) Incoherent, meaningless and/or irrelevant content included in the article
(6) Manipulated or compromised peer review

The presence of these indicators undermines our confidence in the integrity of the article's content and we cannot, therefore, vouch for its reliability. Please note that this notice is intended solely to alert readers that the content of this article is unreliable. We have not investigated whether authors were aware of or involved in the systematic manipulation of the publication process.

Wiley and Hindawi regrets that the usual quality checks did not identify these issues before publication and have since put additional measures in place to safeguard research integrity.

We wish to credit our own Research Integrity and Research Publishing teams and anonymous and named external researchers and research integrity experts for contributing to this investigation.

The corresponding author, as the representative of all authors, has been given the opportunity to register their agreement or disagreement to this retraction. We have kept a record of any response received.

References

[1] C. Liu, "Design and Research of Building Indoor Environment Monitoring System Relying on 3D Modeling and Image Processing," *Journal of Electrical and Computer Engineering*, vol. 2022, Article ID 1386681, 10 pages, 2022.

Hindawi
Journal of Electrical and Computer Engineering
Volume 2022, Article ID 1386681, 10 pages
https://doi.org/10.1155/2022/1386681

Research Article

Design and Research of Building Indoor Environment Monitoring System Relying on 3D Modeling and Image Processing

Chenguang Liu

The Audit Department, Shandong College of Arts, Jinan 250004, Shandong, China

Correspondence should be addressed to Chenguang Liu; z00107@sdca.edu.cn

Received 11 April 2022; Revised 7 May 2022; Accepted 27 May 2022; Published 21 June 2022

Academic Editor: Wei Liu

In order to improve the monitoring effect of building indoor environment, this paper carries out indoor environment simulation through 3D modeling, uses image processing technology to collect environmental monitoring data, and proposes a routing algorithm applied in this environment. Moreover, this paper introduces the energy consumption model of sensor nodes and the multi-attribute decision-making method and uses the multi-attribute decision-making to propose an adaptive energy balance routing algorithm based on the indoor environment of the building. In addition, this paper establishes a simulation analysis, compares it with several other routing algorithms, and verifies that the proposed algorithm has better balance in network energy consumption and longer network life cycle. Finally, this paper combines three-dimensional modeling and image processing technology to construct the building indoor environment monitoring system. It can be seen from the simulation experiments that the proposed building indoor environment monitoring system based on 3D modeling and image processing can meet the actual needs of intelligent building indoor monitoring.

1. Introduction

Smart buildings are a rapidly developing architectural form, and the research focus in the 21st century has begun to shift from technology to user experience. Building intelligence is the core technology for building perception, transmission, and data processing, and the use of building intelligence monitoring and control systems can save 20% of energy consumption. At this stage, the coverage of China's building intelligent system is relatively extensive, which takes into account not only the system construction in new buildings, but also the intelligent transformation of existing buildings. However, relevant research should not be limited to the system design of a single building but should also focus on the development and construction of smart cities and smart buildings, aiming to promote the sustainable development of buildings throughout their life cycle. As the main body of new concepts such as smart city and smart building, in recent years, related research on building intelligence has achieved certain results with the joint efforts of all sectors of society. According to statistics, the energy consumption of major buildings in China has decreased slightly, and the growth rate of total building energy consumption has slowed down. Generalized building energy consumption is divided into building operation energy consumption, building material energy consumption, and building indirect energy consumption. Studies have shown that once a building is built, its operating energy consumption becomes the main evaluation index to measure whether it conforms to the building's green operation.

This paper combines three-dimensional modeling and image processing technology to construct a building indoor environment monitoring system, to promote the further development of intelligent buildings and improve the indoor living experience.

2. Related Work

Active Badge indoor positioning system uses infrared to perform indoor positioning. The system consists of mobile tags, sensors, and servers; the mobile tags continuously emit infrared signals for unique identification around them; the sensor network installed indoors captures the signals emitted by the mobile tags and transmits them to the server; and the server uses the approximate method to estimate the area where the mobile tag is located [1]. However, the Active Badge system can only realize regional discrimination for mobile labels. In order to reduce the positioning error of the infrared positioning system, a large number of light sensors can be deployed indoors and colocated with optical cameras [2]. The Firefly system [3] is a classic indoor positioning system that uses a combination of dense sensors and optical cameras to achieve high-speed real-time optical tracking indoor positioning, and the system positioning accuracy can reach 3 mm. However, because the system uses a camera array, the equipment cost is relatively high; it is necessary to install dense infrared receiving equipment in the indoor area to be tested, which requires a lot of work; in addition, the range covered by the Firefly system is also relatively small.

According to the time it takes for the ultrasonic wave to propagate in the air, the propagation distance can be calculated, so that the ultrasonic wave has also been deeply studied in the field of positioning [4]. The literature [5] uses ultrasonic technology to design Active Bat indoor positioning system. Active Bat system needs to deploy dense signal receiving devices on the ceiling of the space to be tested to detect the signals emitted by mobile tags, and it needs to know the precise position coordinates of each signal receiving device. And each signal receiving device has a unique identifier. The mobile tag transmits ultrasonic waves around the area to be measured, and the pre-deployed signal receiving device detects the signal emitted by the mobile tag and estimates the distance from the mobile tag to the receiving device according to the propagation time of the ultrasonic wave in the air. The coordinate information and the estimated distance between the mobile tag and the receiving device are sent to the central server, and the central server uses the location information of the receiving device and the distance to the tag to estimate the location coordinates of the tag using multipoint technology [6]. Using ultrasound for positioning can achieve high-precision positioning, and the mobile transmitting tag has the advantages of easy portability and low power consumption. However, the indoor positioning system is in a complex indoor environment, and various indoor objects interfere with the positioning system, which increases the positioning error of the positioning system [7].

The Ubisense system [8] is a representative system that uses ultra-broadband technology to achieve indoor positioning; the system consists of three parts: sensor network, mobile positioning tag, and central server. The positioning tag sends pulse signals and is deployed in the indoor sensor network. After receiving the pulse signal, the information is transmitted to the positioning server, and the central server analyzes the received data information to estimate the coordinate information of the user in the area to be measured; using the geometric measurement algorithm to estimate the positioning of the mobile positioning tag, the system can achieve centimeter level of positioning error. Due to the large bandwidth of the UWB pulse signal, the ability to penetrate obstacles is strong, and the signal is not sensitive to the change of the channel, so that the system positioning accuracy is less affected by indoor obstacles [9]. The positioning system using UWB technology can adapt to the indoor environment with high environmental complexity. In China, the research of UWB technology in positioning has also achieved a lot of results. The representative indoor positioning system product is the LocalSense wireless indoor positioning system developed by Tsinghua University [10].

RFID is a noncontact communication technology, which is widely used in the positioning and tracking of moving objects. The SpotON positioning system [11] and WhereNet system are two representative positioning systems designed using RFID. The SpotON system analyzes the signal strength received by the sensor and converts the sensed signal strength into the physical relationship between the tag and the sensor. An aggregation algorithm is used to estimate the position coordinate information of the mobile tag in the area to be measured. The WhereNet system uses active RFID positioning technology, and the system also wears RFID tags on the objects, and the RFID tags actively transmit radio signals to the surrounding area. Multiple receivers deployed indoors capture the radio signals, and the positioning processor is based on the time difference of the signals. Position coordinates the estimation for mobile RFID tags. The positioning accuracy of the system is about 2 m. RFID has the advantages of relatively small size of mobile positioning tags, being easy to carry, and low system cost. However, the effective distance of the RFID positioning system transmitting signals is relatively short. To achieve positioning in large buildings, a large number of signal receivers need to be deployed, and the workload is large. Bluetooth technology utilizes multiple mobile devices to connect to a local area network to realize wireless data exchange in a short distance instead of wired data communication [12]. The Bluetooth indoor positioning system [13] uses mobile Bluetooth devices to connect with devices in the local area network, calculates the distance between devices by calculating the time difference between signal arrivals among devices, and uses geometric measurement algorithms to estimate the indoor coordinate information of mobile devices. .Not only is the positioning system convenient for networking, but it also has the advantage that signal propagation is less affected by non-line-of-sight, which is conducive to large-scale promotion; however, Bluetooth signals are easily affected by the surrounding environment, and the signal propagation distance is relatively short, so the positioning system based on Bluetooth is only suitable for indoor environment with simple environment and small space. WLAN positioning relies on the deployed wireless local area network and smart devices containing wireless receivers to complete positioning. The Ekahau system is a representative positioning system that uses WLAN to achieve positioning in indoor environments [14]. The system can be divided into three parts: mobile positioning tag, network explorer, and positioning server. In the offline stage, the system detects the RSS, SNR, and other information of the network through the network detector and associates the signal strength with the location coordinates of the sampling. The system uses statistical knowledge to estimate the location of the mobile terminal. The positioning accuracy of the Ekahau system is controlled at about 3 m, so the positioning accuracy of the positioning system is not ideal [15].

Vision-based localization systems [16] can intuitively identify the user's form. The system deploys two cameras in the positioning area. The cameras collect data from multiple angles and then transmit the data to the server in real time. According to the received data, the server estimates the position coordinates and attitude of the object in the area to be measured through an effective algorithm. Visual positioning can intuitively display the shape and position information of the positioning object. The camera covers a wide range, and the ideal positioning effect can be achieved without arranging too many cameras in the positioning space [17]. However, the camera is greatly affected by the ambient light; in a dim environment, the positioning accuracy of the system decreases, and the complexity of the image processing algorithm is high, which requires high computing power of the system [18].

3. Basic Algorithm for Design of Building Indoor Environment Monitoring System

There are many factors to be considered in the research of WSN routing protocol, and there are many classification methods according to different standards. Among them, the research on routing protocols classified according to the network topology is of great significance. Routing protocols are classified according to the network topology, including plane routing protocols and hierarchical routing protocols. This section will introduce these two types of protocols and the several typical specific protocols they contain.

The routing algorithm of the SPIN protocol is data-centric, based on a negotiation mechanism, and has energy adaptability. There are three types of communication information in this protocol in network communication: ADV (data description), REQ (data request), and DATA (data). Before sending DATA (data) information, the node will first broadcast ADV information, describing the data to be sent. After that, other nodes that receive the broadcast determine whether they need to receive the next data according to the data description. The nodes that meet the data description will send a REQ message in response, respond to the data request node, and then wait to receive data. The SPIN protocol adopts a negotiation mechanism and can purposefully transmit data through data description, which avoids many problems such as information explosion, information duplication, and resource waste and overcomes these shortcomings in the Flooding and Grossing protocols. The routing establishment and data transmission process of the SPIN protocol is shown in Figure 1.

The SPIN protocol does not consider the issue of energy saving, nor does it address the problem of data transmission under various channel conditions. The indoor environment is unstable and dynamic, and it is difficult for the SPIN protocol to ensure the stability of the transmission link and the reliable transmission of data.

The process of selecting cluster heads in LEACH algorithm is as follows. First, all nodes will randomly generate a number between 0 and 1 and calculate the probability T_n of being selected as the cluster head in this round according to the formula shown in (1). After that, the algorithm compares T_n with the generated random number. If the random number is less than T_n, the node is selected as the cluster head, and the node publishes the message that it has become the cluster head. In each round of cluster head selection, the node that has been selected as the head node will set T_n to 0 to avoid being selected as the cluster head again in this round. T_n represents the election probability of the node that has not yet been elected as the cluster head. According to (1), the probability T_n of remaining nodes being elected as cluster head nodes will increase with the increase of nodes elected as cluster head nodes in the network. The larger T_n, the greater the probability of generating a random number smaller than T_n, and the greater the probability of becoming a cluster head.

$$T_n = \begin{cases} \dfrac{p}{1 - p\,(r \bmod 1/p)}, & n \in G, \\ 0, & \text{other}. \end{cases} \tag{1}$$

In (1), p represents the percentage of the total number of cluster heads in the number of all nodes in the entire network. $r\bmod(1/P)$ represents the number of cluster head nodes that have been elected in this round, r represents the number of election rounds, and G represents the set of nodes that have not yet been elected as cluster heads in this round. The node selected as the cluster head broadcasts the message to become the cluster head. After the non-cluster head node in the network receives the cluster head message, it selects the node with the strongest received signal strength, sends a request message, and joins the cluster head.

LEACH selects a new cluster head in a random way and does not fully consider the remaining energy of nodes. In this way, nodes with lower energy still have a higher probability of being selected as the cluster head. When nodes with low energy are still selected as cluster heads, the energy of these nodes will be depleted prematurely. Moreover, in the LEACH protocol, the cluster head communicates directly with the sink node, and there are a lot of barriers in the building environment. Therefore, such a communication method will further accelerate the energy consumption of the cluster head, reduce the energy consumption balance of the network, and shorten the network life cycle.

The energy consumption of sensor nodes includes data transmission energy consumption, data reception energy consumption, and data fusion energy consumption. Among them, the energy consumption of data transmission consists of two parts: the energy consumption of the transmitting circuit and the energy consumption of the power amplifier circuit. The data of the length of l bits is sent between the two nodes, and the energy consumed by the sending distance d is calculated as the following formula:

$$E_t(l, d) = \begin{cases} lE_{elec} + l\varepsilon_{f_f} d^2, & d < d_T, \\ lE_{elec} + l\varepsilon_{mp} d^4, & d \geq d_T. \end{cases} \tag{2}$$

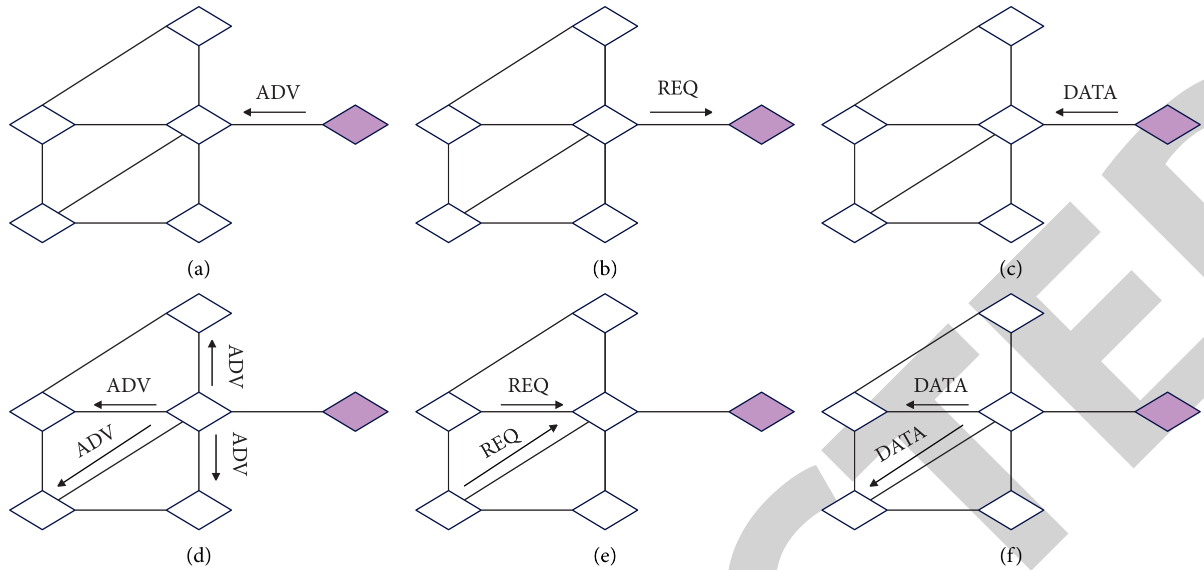

FIGURE 1: SPIN protocol working process. (a) Broadcasting ADV. (b) Data request. (c) Sending data. (d) Broadcasting ADV. (e) Data request. (f) Sending data.

In the formula, d_T is the threshold that determines the selection of the two energy models, and the calculation of the threshold is shown in (3). When d is less than the threshold d_T, the energy consumption calculation of data transmission adopts the free space model. When d is greater than or equal to the threshold d_T, the multipath fading model is used to calculate the energy consumption of data transmission. E_{elec} is the circuit energy consumption of transmitting or receiving unit bit data, ε_{fs} and ε_{mp} are the energy amplification coefficients of the power amplifier circuit.

$$d_T = \sqrt{\frac{\varepsilon_{fs}}{\varepsilon_{mp}}}. \tag{3}$$

When the sensor node receives data with a length of l bits, the energy consumption calculation formula is as follows:

$$E_r(l) = lE_{elec}. \tag{4}$$

When the sensor node fuses data with a length of l bits, the energy consumption calculation formula is as follows:

$$E_a(l) = lE_{da}. \tag{5}$$

In the formula, E_{da} represents the circuit energy consumption of fusing unit bit data.

When the sensor node is monitoring, the energy consumption is roughly the same as the energy consumption when receiving data. The monitoring energy consumption can be calculated according to the energy consumption coefficient of the received data. The calculation formula is as follows:

$$\text{Eil}(l) = lE_{elec}. \tag{6}$$

In the experiment, the parameter lE_{elec} is set to 50 nJ/bit, the parameter ε_{fs} is 10 pJ/bit/m^2, the parameter ε_{mp} is 0.0013 pJ/bit/m^4, and the parameter E_{da} is 5 nJ/bit.

The multi-attribute decision-making model not only considers multiple attributes of the system model, but also uses the subjective and objective weight coefficients to reflect the importance of different attributes. Moreover, it can realize more accurate decision-making for the dynamic indoor environment, better realize the routing algorithm for the indoor wireless sensor network, and improve the energy balance effect of the network. Formula (7) defines the multi-attribute decision-making model:

$$\max_{j=1\ldots m}\text{MAD} = \sum_{k=1}^{\text{num}} \left(\beta \cdot w_k + (1-\beta)\cdot w_k'\right)\cdot u_{jk},$$
$$\text{s.t.}\begin{cases} \sum_{k=1}^{\text{num}} w_k = 1, & \sum_{k=1}^{\text{num}} w_k' = 1, \\ 0 \le w_k \le 1, & 0 \le w_k' \le 1, \\ 0 \le \beta \le 1, & u_{jk} \ge 0, \\ \text{num} \ge 1, & \text{num} \in N. \end{cases} \tag{7}$$

In (7), MAD is the result of multi-attribute decision-making, u_{jk} represents the k-th normalized attribute in the j-th neighbor node, and m represents the number of neighbor nodes. num represents the number of evaluation attributes, w_k represents the subjective weight coefficient, w_k' is the objective weight coefficient, and β represents the ratio of the subjective weight coefficient.

3.1. Normalized Attribute u_{jk}.

Each sensor node contains an attribute matrix A, as shown in the following formula:

$$A = \begin{bmatrix} U_{11} & U_{12} & \cdots & U_{1\text{num}} \\ U_{21} & U_{22} & \cdots & U_{2\text{num}} \\ \vdots & & & \\ U_{m1} & U_{m2} & \cdots & U_{m\text{num}} \end{bmatrix}. \tag{8}$$

Among them, the row vector of the matrix represents the num different evaluated attribute values of the neighbor nodes of the node, and the column vector is the attribute vector. A_i is the attribute vector of the i-th attribute of the m neighbor nodes of the sensor node. The dimension and order of magnitude of each evaluation attribute are different. Before making a decision, the attribute matrix needs to be normalized. In the normalization process, the optimal solution U_i^* and the negative optimal solution $\overline{U_i^*}$ of the i-th attribute of the node need to be calculated first, and the calculation formula is as shown in (9). Then, we calculate the normalized value of the i-th attribute of each node according to (10) and denote the i-th normalized attribute value of the j-th node as u_{jk}. Finally, the normalized matrix B is obtained, as shown in (11).

The optimal solution U_i^* and the negative optimal solution $\overline{U_i^*}$ are computed:

$$\begin{aligned} U_i^* &= \mathrm{Max}(A_i), \\ \overline{U_i^*} &= \mathrm{Min}(A_i). \end{aligned} \tag{9}$$

The normalization processing formula of the i-th attribute of the j-th node is as follows:

$$u_{ji} = \frac{U_{ji} - \min A_i}{\max A_i - \min A_i}. \tag{10}$$

The normalized attribute matrix B is as follows:

$$B = \begin{bmatrix} u_{11} & u_{12} & \cdots & u_{1\mathrm{num}} \\ u_{21} & u_{22} & \cdots & u_{2\mathrm{num}} \\ \vdots & \vdots & \vdots & \vdots \\ u_{m1} & u_{m2} & \cdots & u_{m\mathrm{num}} \end{bmatrix}. \tag{11}$$

The normalization process avoids the influence of the dimensional differences of various evaluation attributes on the decision-making results and improves the accuracy of the multi-attribute decision-making results.

3.2. Objective Weight Coefficient w_k'.

The objective weight coefficient refers to the coefficient that is only affected by objective factors, that is, the evaluation attributes, in the decision-making process. The entropy of the system is defined by (12). Entropy has extreme value. When the probability of each attribute in the system is the same, the entropy value is the largest. Therefore, for each different neighbor node, the smaller the difference in an attribute, the greater the attribute entropy value. The k-th attribute probability p_j^k in node j is calculated from this property of entropy, as in (13). The entropy of a system is defined as follows:

$$E = -\sum_{j=1}^{m} p_j \log p_j. \tag{12}$$

The k-th attribute probability of node j is as follows:

$$p_j^k = \frac{u_{jk}}{\sum_{j=1}^{m} u_{jk}}. \tag{13}$$

The calculation of the entropy value of the k-th attribute is as follows:

$$H_k = -\sum_{j=1}^{m} p_j^k \log p_j^k. \tag{14}$$

By normalizing the attribute entropy value and taking $u_{jk} = 0$, $p_j^k \log p_j^k = 0$. The entropy value H_k is normalized to calculate the relative value h_k:

$$h_k = \frac{H_k}{H_k^{\max}}. \tag{15}$$

Among them, $H_k^{\max}$ is the maximum value of the entropy value:

$$H_k^{\max} = -\sum_{j=1}^{m} \frac{1}{m} \log \frac{1}{m} = \log m. \tag{16}$$

Using the calculated relative entropy value to calculate the objective weight coefficient, the calculation formula is as follows:

$$w_k' = \frac{1 - h_k}{\mathrm{num} - \sum_{k=1}^{\mathrm{num}} h_k}. \tag{17}$$

The objective weight coefficient satisfies $0 \le w_k' \le 1$ and $\sum_k^{\mathrm{num}} w_k' = 1$, and the objective weight coefficient reflects the relative fierceness of the internal competition of each attribute and represents the amount of effective information of the corresponding attribute in decision-making.

3.3. Subjective Weight Coefficient w_k.

Sensor nodes have many different attributes, each attribute has a different proportion to decision-making, and the subjective weight coefficient is the embodiment of the designer's subjective importance to different attributes in the algorithm design. The subjective weight coefficients of these attributes are combined into a set $w = (w_1, w_2, \ldots, w_k, \ldots, w_l)$ of subjective weight coefficients. In the algorithm design, the importance of attributes in the system is adjusted by subjectively modifying the weight coefficients of different attributes to achieve the optimal routing effect.

3.4. Ratio of Subjective and Objective Weighting Coefficients β.

The model includes subjective weights and objective weights. In the decision-making process, the two weights need to be allocated in a proportion, and the ratio of the subjective and objective weight coefficients β is the proportion of this allocation. This ratio reflects the weighting degree of the two weights in decision-making. If $\beta = 1$, the effect of the objective weight coefficient is not considered in the decision, and the decision result is completely determined by the subjective weight coefficient. Such a routing algorithm is called subjective weight routing. If $\beta = 0$, the decision result is completely determined by the objective weight coefficient. Such a routing algorithm is called objective weight routing.

Based on the previously analyzed building indoor environment and routing algorithm, this paper uses the multi-attribute decision-making model proposed above to analyze the specific steps of the building indoor routing algorithm as follows:

(1) Initial stage.
(2) Establishing candidate head node set and neighbor node set stage.
(3) Cluster selection and forwarding node stage.
(4) The non-cluster head forwarding node selecting the route forwarding node stage.
(5) Cluster establishment stage.
(6) Data stable transmission stage.

The RF transmit power of a node can be set to different levels, and different RF transmit powers correspond to different network transmission ranges. The transmission power of nodes is related to the range of network clustering and the size and balance of network energy consumption. Here, different node transmission ranges are set for simulation, and the influence of node transmission range on network life cycle and network energy balance is analyzed. Figures 2 and 3 show the network life cycle and the relationship between the standard deviation of the node's remaining energy and the node's transmission range.

The simulation results of Figures 2 and 3 show that when the transmission range is increasing, the network life cycle is decreasing and the standard deviation of the remaining energy of the network nodes is increasing. When the transmission range distance is 15 m, the network has the longest network lifetime and the smallest node residual energy standard deviation. At this time, the network energy consumption is the most balanced, and the performance of the algorithm is optimal.

In the process of clustering using the clustering routing algorithm, a multi-attribute decision-making model is used to select the cluster head. In the algorithm, the node residual energy E_i and RSSI loss value are selected as decision attributes. The cluster head node receives data packets, fuses the data, routes and forwards the data, and consumes a lot of energy in the system, which directly affects the network energy balance consumption and the network life cycle. Since there is a relationship between the RSSI loss value and the subjective weight coefficient of the node's remaining energy: $W_{E\_CH} + W_{RSSI\_CH} = 1$, it is enough to analyze the influence of only one of the variables on the energy balance of the network. Figures 4 and 5 present the relationship between the node residual energy standard deviation, the network life cycle, and the node residual energy subjective weight coefficient.

It can be seen from Figures 4 and 5 that when W_{E_CH} is between 0.6 and 0.85, the standard deviation of the residual energy of the node is small, the variation range is small, and the network life cycle is long. In the process of increasing W_{E_CH} from 0.5, the standard deviation of the node residual energy gradually decreases, the energy distribution becomes more and more balanced, and the network life cycle becomes longer and longer. When the coefficient increases from 0.5, the standard deviation of the node residual energy gradually decreases, and the energy distribution becomes more and more balanced, which also shows that the node residual energy has a greater impact on the network balance in the process of cluster head selection. When the remaining energy is almost taken as the main consideration condition,

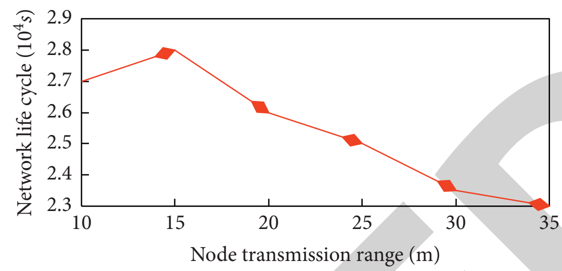

Figure 2: Relationship between network life cycle and node transmission range.

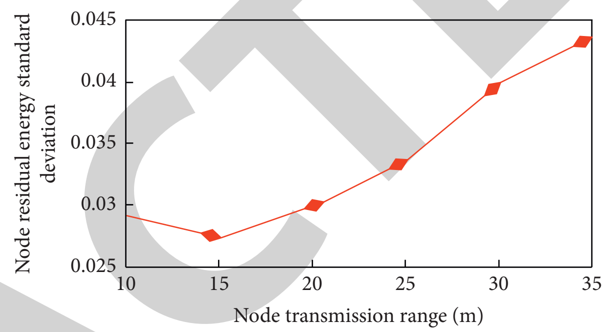

Figure 3: The relationship between the standard deviation of the residual energy of the node and the transmission range of the node.

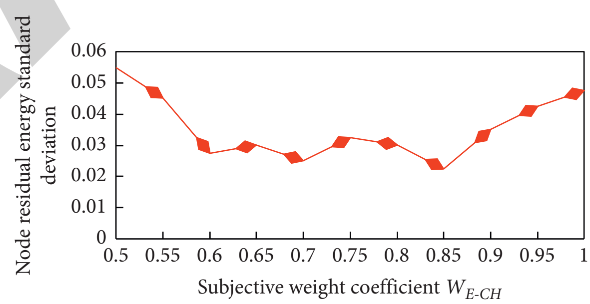

Figure 4: The change relationship between the residual energy of the node and the subjective weight coefficient W_{E_CH}.

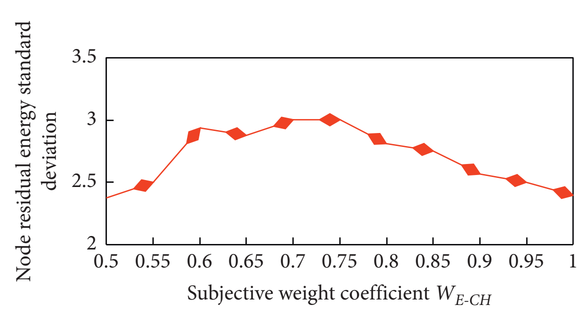

Figure 5: The change relationship between the network life cycle and the subjective weight coefficient W_{E_CH}.

because the energy loss from the cluster head to the sink node is not fully considered, the energy consumption of the cluster head increases in the process of forwarding data. At this time, the energy balance of the network begins to decline, and the network life cycle is shortened, which also verifies the importance of using the multi-attribute decision-making model to the algorithm.

When designing a WSN routing algorithm, in order to improve the network life cycle, the routing algorithm needs to take energy consumption balance as a major consideration. The network life cycle reflects the effectiveness of the overall energy utilization of the network. The longer the network life cycle, the more balanced and efficient the network energy utilization is. The network runtime when the first dead node appears is defined as the network lifetime. Figure 6 is a comparison of the simulation results of the network life cycle of several common routing algorithms and the routing algorithm proposed in this paper.

The standard deviation of the remaining energy of a node directly reflects the energy balance of each node in the network. The smaller the standard deviation, the higher the balance of energy consumption in the network. Figure 7 shows the standard deviation of residual energy of network nodes for several algorithms. The results in the figure show that the routing algorithm designed in this paper has the smallest standard deviation among several algorithms, and the network energy consumption is the most balanced. Moreover, with the increase of the number of experimental rounds, the standard deviation of the residual energy of the network changes little, which proves the energy balance of the algorithm.

The whole monitoring platform mainly includes two parts: the upper computer monitoring center and the building indoor environmental parameter acquisition system based on ZigBee wireless network. The host computer is responsible for the collection and processing of indoor environment data to provide monitoring of the indoor environment and also includes the control of ZigBee wireless network. From the perspective of system structure, it can be divided into three layers, the first layer is the monitoring center, the second layer is the information aggregation layer, and the third layer is the information perception layer. The environmental information perception layer is responsible for perceiving environmental attributes and transmitting the perception data to the information aggregation layer, and the aggregated information is then transmitted to the monitoring center to complete the real-time monitoring of the monitoring area environment.

The overall frame structure of the system is shown in Figure 8.

4. Building Indoor Environment Monitoring System Relying on 3D Modeling and Image Processing

The third section presents the wireless sensing algorithm for indoor monitoring in this paper. On this basis, a building indoor environment monitoring system based on image processing and indoor 3D modeling technology is constructed. This paper relies on image processing and indoor 3D modeling technology for data collection and combines the data processing and transmission algorithms in the third part for data processing and transmission.

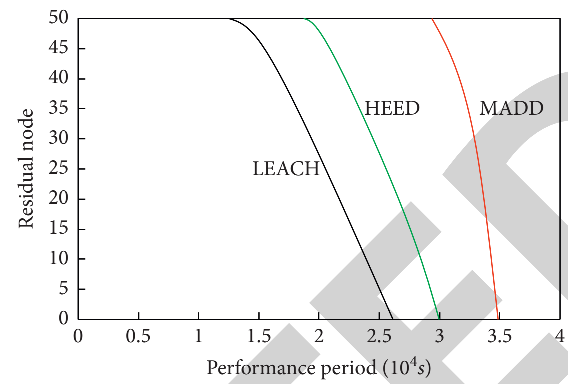

Figure 6: Comparison of network life cycles of different routing algorithms.

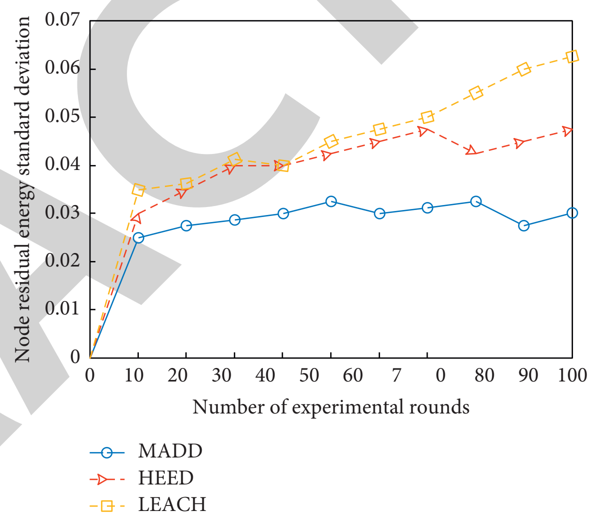

Figure 7: Comparison of residual energy standard deviation of network nodes with different algorithms.

This paper presents the functional module division scheme of the system. The specific function division is shown in Figure 9. The entire indoor environment monitoring system consists of four independent sub-applications, namely, the collector program, the App application, the server-side application, and the client-side application. Among them, the blue-colored is the function already existing in the original system.

On the basis of the indoor environment monitoring system constructed above, this paper verifies the effect of the model through a simulation test. The test platform of this paper is Matlab, the test is carried out on this platform to evaluate the data collection and environmental monitoring effect of the system in this paper, and the results shown in Table 1 are obtained.

It can be seen from the above research that the proposed building indoor environment monitoring system based on 3D modeling and image processing can meet the actual needs of intelligent building indoor monitoring.

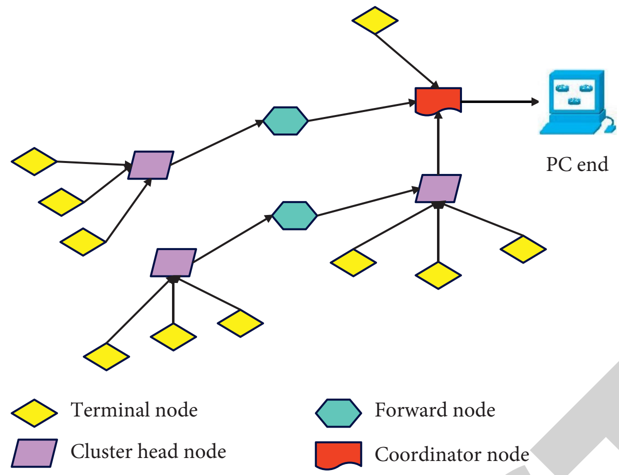

Figure 8: Overall frame structure of the system WSN.

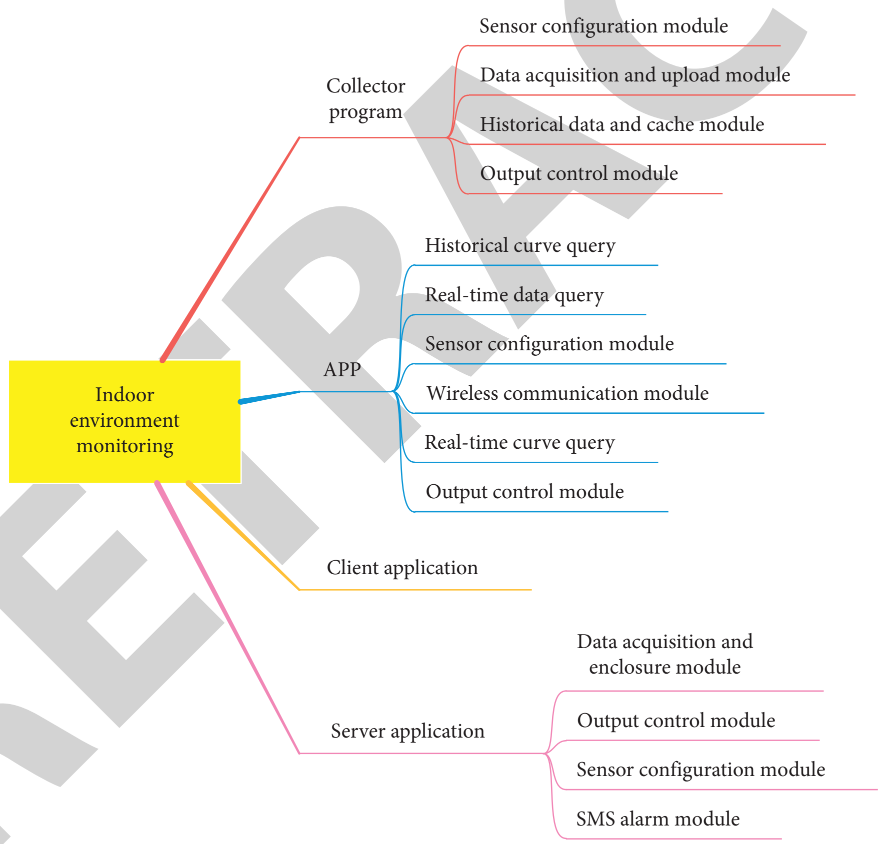

Figure 9: System function module division diagram.

Table 1: The data collection and environmental monitoring simulation effects of the system in this paper.

Number	Data collection	Environmental monitoring	Number	Data collection	Environmental monitoring	Number	Data collection	Environmental monitoring
1	89.25	76.81	18	90.42	77.66	35	92.69	75.93
2	93.21	74.24	19	93.63	79.64	36	91.90	79.03
3	88.52	80.05	20	93.32	75.97	37	90.40	73.09
4	91.92	78.64	21	90.65	80.73	38	91.83	76.15
5	89.24	78.37	22	89.12	72.02	39	91.36	81.29
6	90.43	81.76	23	90.13	74.22	40	92.47	70.75
7	90.57	78.25	24	90.17	77.64	41	90.83	76.40
8	91.04	70.61	25	89.22	77.62	42	92.08	70.99
9	90.32	76.75	26	89.23	72.40	43	88.25	72.53
10	92.79	81.55	27	92.22	79.61	44	89.47	77.32
11	88.67	80.06	28	88.52	74.76	45	92.31	81.27
12	93.94	77.23	29	94.00	69.68	46	93.77	82.76
13	92.68	73.43	30	89.34	76.49	47	90.78	82.85
14	88.08	78.88	31	91.57	79.91	48	88.72	68.26
15	90.67	70.24	32	91.83	73.72	49	88.71	73.96
16	88.69	70.07	33	92.56	79.42	50	93.44	79.39
17	88.34	79.24	34	93.50	70.10	51	88.62	83.41

5. Conclusion

Building an intelligent system is an important means to realize building operation monitoring. It can effectively reduce the energy consumption of various kinds of equipment and ensure that the building is more efficient and energy saving throughout its life cycle. In order to facilitate system integration and unified management and control of operation and maintenance personnel, this paper combines the Internet of Things, big data, and cloud computing technologies to build a building information management platform. From hardware development to software development, existing building networking systems have basically fulfilled various requirements such as monitoring, control, and optimization. With the continuous advancement of technology, the modular building networking system is becoming more and more perfect, but it still shows certain limitations at this stage. This paper combines three-dimensional modeling and image processing technology to construct a building indoor environment monitoring system. Through the simulation test, it can be seen that the building indoor environment monitoring system relying on three-dimensional modeling and image processing proposed in this paper can meet the actual needs of intelligent building indoor monitoring.

Data Availability

The labeled dataset used to support the findings of this study is available from the author upon request.

Conflicts of Interest

The author declares no conflicts of interest.

Acknowledgments

This study was sponsored by Shandong College of Arts.

References

[1] H. R. Abed, W. A. Hatem, and N. A. Jasim, "Adopting BIM technology in fall prevention plans," *Civil Engineering Journal*, vol. 5, no. 10, pp. 2270–2281, 2019.

[2] Y. Y. Al-Ashmori, I. Othman, Y. Rahmawati et al., "BIM benefits and its influence on the BIM implementation in Malaysia," *Ain Shams Engineering Journal*, vol. 11, no. 4, pp. 1013–1019, 2020.

[3] C. J. Chen, S. Y. Chen, S. H. Li, and H. T. Chiu, "Green BIM-based building energy performance analysis," *Computer-Aided Design and Applications*, vol. 14, no. 5, pp. 650–660, 2017.

[4] A. Dainty, R. Leiringer, S. Fernie, and C. Harty, "BIM and the small construction firm: a critical perspective," *Building Research & Information*, vol. 45, no. 6, pp. 696–709, 2017.

[5] M. O. Fadeyi, "The role of building information modeling (BIM) in delivering the sustainable building value," *International Journal of Sustainable Built Environment*, vol. 6, no. 2, pp. 711–722, 2017.

[6] L. Joblot, T. Paviot, D. Deneux, and S. Lamouri, "Literature review of Building Information Modeling (BIM) intended for the purpose of renovation projects," *IFAC-PapersOnLine*, vol. 50, no. 1, pp. 10518–10525, 2017.

[7] I. Kim, J. Choi, E. A. L. Teo, and H. Sun, "Development of K-BIM e-Submission prototypical system for the openBIM-based building permit framework," *Journal of Civil Engineering and Management*, vol. 26, no. 8, pp. 744–756, 2020.

[8] M. N. Kocakaya, E. Namli, and U. Isikdag, "Building information management (BIM), a new approach to project management," *Journal of sustainable construction materials and technologies*, vol. 4, no. 1, pp. 323–332, 2019.

[9] A. Koutamanis, J. Heuer, and K. D. Könings, "A visual information tool for user participation during the lifecycle of school building design: bim," *European Journal of Education*, vol. 52, no. 3, pp. 295–305, 2017.

[10] T. Mandičák, P. Mesároš, and M. Tkáč, "Impact of management decisions based on managerial competencies and skills developed trough BIM technology on performance of

construction enterprises," *Pollack Periodica*, vol. 13, no. 3, pp. 131–140, 2018.
[11] S. M. Noor, S. R. Junaidi, and M. K. A. Ramly, "Adoption of building information modelling (bim): factors contribution and benefits," *Journal of Information System and Technology Management*, vol. 3, no. 10, pp. 47–63, 2018.
[12] A. Okakpu, A. GhaffarianHoseini, J. Tookey, J. Haar, A. Ghaffarianhoseini, and A. Rehman, "A proposed framework to investigate effective BIM adoption for refurbishment of building projects," *Architectural Science Review*, vol. 61, no. 6, pp. 467–479, 2018.
[13] E. Papadonikolaki, C. van Oel, and M. Kagioglou, "Organising and managing boundaries: a structurational view of collaboration with building information modelling (bim)," *International Journal of Project Management*, vol. 37, no. 3, pp. 378–394, 2019.
[14] L. Ustinovichius, V. Popov, J. Cepurnaite, T. Vilutienė, M. Samofalov, and C. Miedziałowski, "BIM-based process management model for building design and refurbishment," *Archives of Civil and Mechanical Engineering*, vol. 18, no. 4, pp. 1136–1149, 2018.
[15] L. Ustinovičius, A. Puzinas, J. Starynina, M. Vaišnoras, O. Černiavskaja, and R. Kontrimovičius, "Challenges of BIM technology application in project planning," *Engineering Management in Production and Services*, vol. 10, no. 2, pp. 15–28, 2018.
[16] T. Wei and Y. Chen, "Green building design based on BIM and value engineering," *Journal of Ambient Intelligence and Humanized Computing*, vol. 11, no. 9, pp. 3699–3706, 2020.
[17] P. Wu, R. Jin, Y. Xu, F. Lin, Y. Dong, and Z. Pan, "The analysis of barriers to bim implementation for industrialized building construction: a China study," *Journal of Civil Engineering and Management*, vol. 27, no. 1, pp. 1–13, 2021.
[18] J. Xu, B. K. Li, and S. M. Luo, "Practice and exploration on teaching reform of engineering project management course in universities based on BIM simulation technology," *Eurasia Journal of Mathematics, Science and Technology Education*, vol. 14, no. 5, pp. 1827–1835, 2018.